Secondary Radical Formation and Electron Spin Polarization in Systems Involving Phosphonyl Radicals

Keith A. McLauchlan * and Nigel J. K. Simpson
Physical Chemistry Laboratory, South Parks Rd., Oxford, OX1 3QZ

Addition of electron spin polarized primary phosphonyl radicals to carbon–carbon double bonds yields secondary radicals the chemical identity of which is obtained from the analysis of the hyperfine structure of their ESR spectra. These radicals exhibit spin polarization (CIDEP) characteristic of a polarization transfer process. The CIDEP patterns reveal the relative signs of the hyperfine couplings in the primary and secondary species. The spectra also exhibit the effects of hyperfine-dependent relaxation unusually clearly, from which the relative signs of the couplings may, in principle, be obtained in these secondary radicals also. Further reaction of the secondary radical to form a tertiary one sometimes also occurs, again with polarization transfer. An example is given of an instance in which a difference in the signs of the coupling constants in these two species leads to a phase reversal in the spectrum of the polarized tertiary radical as a result of this process.

Flash photolysis ESR is a well established method for obtaining the chemical identities of very short-lived free radicals in solution. The radicals observed within the first few microseconds of their creation commonly exhibit ESR spectra which display the effects of spin polarization, CIDEP.[1] In the first instance, this confers a greater intensity to the signals, and makes transient species easier to observe. In the second, the spectra of primary radicals exhibit relative and absolute intensities of their hyperfine components which disclose the spin multiplicity of the molecular precursor the reaction of which leads to radical formation. In this paper we are concerned mostly with the radical pair mechanism (RPM) where these primary species are concerned. This produces a population dis-equilibrium between the various hyperfine states of the radicals, and leads to characteristic spectral features; in the common ST_0 form of this process the halves of the spectrum of a pair of identical radicals appear with equal intensities in opposite phases. In general, however, the total intensities of the lines in the two different phases differ, either as a result of the radicals differing, in RPM polarization, or because a single-phase contribution results from the triplet mechanism of CIDEP, or both; furthermore a contribution from ST_{-1} RPM effects may be evident. It has been realized for some time that reaction of a polarized primary radical with a molecule, within the spin-lattice relaxation time of the primary and with conservation of electron spin orientation, preserves the spin dis-equilibrium in the system and leads to the formation of a spin-polarized secondary species.[2,3] This implies that polarization may be used as a non-intrusive label for following a reaction pathway of the primary radical to form further generations of radicals.[4] This principle is applied here in a study of phosphonyl radical addition to molecules which contain carbon–carbon double bonds, the system being chosen so as to allow a detailed interpretation of the polarization characteristics observed in the secondary species. Furthermore, the choice allows us to make use of previous product-formation studies[5] on similar systems.

The nature of the CIDEP observed in secondary radicals depends on whether or not hyperfine couplings are correlated between the parent and daughter species. If not, an excess of α spin, for example, in the primary, due to the possible asymmetry in the polarization referred to above, becomes distributed at random over all the hyperfine states of the secondary.[2,3] The spectrum then appears in net emission, with no distortion of the relative intensities of the individual hyperfine components as compared with those from the same radicals observed at thermal equilibrium. A full theoretical analysis has been made of this case, but its results have yet to be applied quantitatively.[6] A more interesting behaviour results if the electron remains coupled to the same nucleus, or nuclei, in the two radicals. As predicted theoretically[7] and recently confirmed,[8] novel polarization patterns may result from which, among others, the relative signs of the coupling constants in the two radicals may be obtained. An example in which the phases of the halves of the spectrum change between the two species as a result of a difference in this sign is provided here for the first time. After their formation, the random encounter of secondary radicals during their free diffusion in solution yields further spin polarization, according to a normal RPM ('F-pair') process. The spectrum observed from the secondary radical consequently displays the simultaneous effects of transfer polarization from the primary and this additional RPM contribution.

The analysis of our experiments depends upon a clear understanding of the polarization phenomena observed, and we first summarize the necessary principles.

Theory.—The origin of RPM polarization in radicals observed immediately after their formation lies in their pairwise geminate formation, with conservation of overall spin multiplicity, on reaction of a molecular precursor. This creates a spin-correlated radical pair which, in the magnetic field of the ESR spectrometer, may exist in singlet (S) or triplet (T_0 or $T_{\pm 1}$) states. Spin polarization results from the spin-evolution of the original spin state in time, under the influence of local magnetic fields, and the action of the electron exchange interaction on the resulting mixed state. Under most conditions only ST_0 mixing is effective, and theoretical analysis then predicts that the halves of the total spectrum relative to the centre should be of opposite phase. For radicals formed from a triplet precursor the spectrum is in emission at low field and in absorption at high, an E/A pattern; the converse is true if the precursor is a singlet state. The population distribution leading to the former is depicted in an energy level diagram corresponding to the electron coupling to a single spin-1/2 nucleus in Figure 1(*a*). With the neglect of a small coupling to the γ protons, this corresponds to the situation in the phosphonyl radicals used as the primary species in this study. In practice too, the spectra of radicals with large coupling constants, such as phosphonyls (see below), may exhibit a further contribution to CIDEP from ST_{-1}

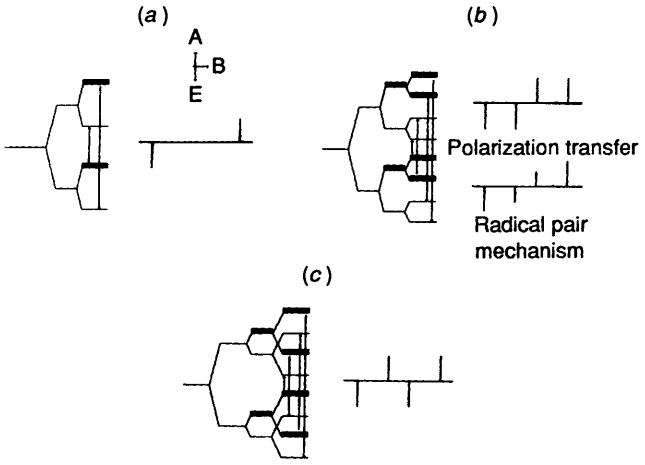

Figure 1. (*a*) The relative level populations, and predicted resultant spectrum, expected for a system in which the electron is coupled to a single spin-1/2 nucleus, such as ^{31}P, in a radical created with E/A spin polarization as one of a pair of identical radicals. (*b*) The corresponding diagrams when this radical forms a secondary species in which the electron becomes coupled to a second spin-1/2 nucleus, such as ^{1}H, whilst remaining coupled to the first; also shown is the spectrum which would be observed if polarization was due to an ST_0 RPM process. It is assumed that the coupling to the original nucleus remains the higher in the secondary radical. (*c*) As in (*b*), but with the original coupling now the smaller of the two. Attention is drawn to the relatively high intensities of the central lines in (*b*), as compared with the RPM predictions, and to the mixtures of phases in the high and low field regions in (*c*). These diagrams were drawn assuming that the couplings are of the same sign.

mixing.[9,10] For the case of a triplet precursor, this causes a net overpopulation of the upper electron spin state leading to a spectrum which exhibits net emission, with some hyperfine-dependence of line intensities. This extra contribution will be neglected for simplicity in the qualitative discussion of the appearance of the spectra of secondary radicals below, but it has been included in the simulated spectra shown in the Results section.

The polarization created in encounters of freely diffusing radicals (in F-pairs) normally also results in E/A patterns in the spectra, and here only ST_0 polarization is significant since the radicals are carbon centred, and exhibit relatively low hyperfine couplings. As with the geminate polarization, its effects on the relative intensities of the various hyperfine components are calculated according to a $Q^{1/2}$-dependence, ensemble-averaged, where Q is a matrix element corresponding to mixing of the S and T_0 states of the radical pair.[11]

When a radical with the population distribution shown in Figure 1(*a*) adds to a double bond, and the electron becomes coupled to a second spin-1/2 nucleus whilst remaining coupled to the first, the energy levels and populations depicted in Figure 1(*b*) and (*c*) may result. In the present case involving the phosphonyl radical, the phosphorus coupling becomes much smaller in the secondary than in the primary radical since the new radical formed now has the electron localized on a carbon atom. Figure 1(*b*) shows the situation where the phosphorus coupling nevertheless remains the greater of the two couplings. Here, the low-field half of the spectrum of the secondary is predicted to be in emission, and the high-field half in absorption, but (in this system of singly degenerate levels) the lines of the spectrum are equal in intensity. This contrasts with the RPM polarization pattern due to ST_0 effects in the encounter of two identical secondary radicals in which the $Q^{1/2}$-dependence causes the central lines to be weakest. The spectra corresponding to these two cases are shown in the diagram, and it is obviously possible to distinguish the two polarization origins in an experiment although, as stated above, F-pair polarization eventually contributes to the observed spectrum as time evolves after radical creation. In the second situation [Figure 1(*c*)], the phosphorus coupling is smaller than to the second nucleus and the spectrum acquires a novel appearance in which (in this simple case) successive lines are of opposite phase. Such behaviour has been demonstrated in just one system previously.[8] Once more the lines are predicted to be of equal intensity before the subsequent F-pair contribution is evident.

The energy levels shown in the diagrams have been labelled, and the derived theoretical spectra drawn, on the assumption that the two hyperfine couplings are of the same sign in the secondary radical as was the single coupling in the primary. If this is not so, the level ordering changes, and the reaction of an E/A-polarized primary radical may lead to a phase-inverted A/E pattern in the spectrum of the secondary. This enables the relative signs of coupling constants in different radicals to be compared. It also indicates that care must be taken to identify one species as a secondary radical, for if it is thought to be a primary one the phase of the spectrum would be interpreted erroneously as indicating a singlet reaction pathway.

Experimental

Spectra were recorded using the Time Integration Spectroscopy (TIS) method[12] in which the signals are detected directly, without the use of field modulation and phase-sensitive detection. The signals are consequently pure absorption ones in the magnetic resonance sense and their phases result from CIDEP effects only. The radicals were produced within the cavity of the ESR spectrometer by irradiating flowing solutions with pulses of 308 nm wavelength light from an excimer laser.

The primary species were created by photolysis of di-*tert*-butyl peroxide, which had been dried over anhydrous sodium sulphite, in the presence of dimethyl or diethyl phosphite (purity > 99%; misleading complications were experienced with less pure materials). To assist solution of the dimethyl compound, methylene dichloride was added as a third component to some of the solvent mixtures. Two stock solutions were used, a 1:1 v/v mixture of peroxide with the diethyl compound, and a corresponding 10:10:3 mixture with the dimethyl compound and methylene chloride, with the latter at the lowest concentration. The peroxide and the phosphites were degassed thoroughly under vacuum before use, and the stock solutions were stored under oxygen-free nitrogen to prevent oxygen re-dissolving during the experiments. To these solutions were added in turn various scavengers which were all used as supplied in their purest commercially available forms (>99.5%). The basic nature of the solutions was controlled by addition of sodium methoxide, chosen since it is not itself photoactive at the laser wavelength and appeared not to induce significant base-catalysed (*e.g.* Michael-like) reaction at the concentrations used.

Results

The primary process in the production of free radicals in the systems studied was the scission of the O–O bond in the peroxide to form a pair of *tert*-butoxy radicals, Scheme 1. These

$$Me_3C\text{–}O\text{–}O\text{–}CMe_3 \xrightarrow{h\nu} 2\ Me_3C\text{–}O^{\bullet}$$

Scheme 1.

radicals could not be observed even at the earliest times after radical formation in our apparatus (*ca.* 30 ns post flash) due to

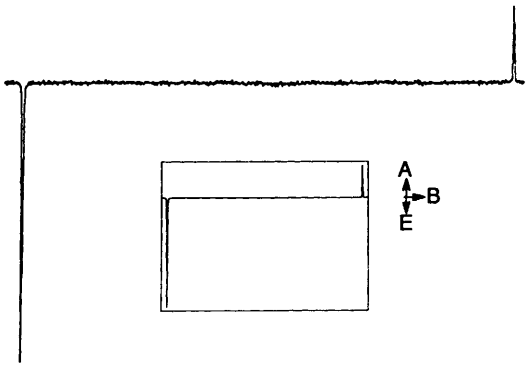

Figure 2. The spectrum of the ethyl phosphonyl radical, and its simulation, obtained on photolysis of the appropriate stock solution, with measurement from 1.0–2.0 μs post the photolysis flash. The spectrum exhibits excess intensity in emission as a result of an ST_{-1} contribution to the polarization, and the simulation was performed by adding the basic ST_0 and ST_{-1} contributions from pairs of similar radicals in the ratio required to reproduce the observed spectrum. The sweep width was 74 mT.

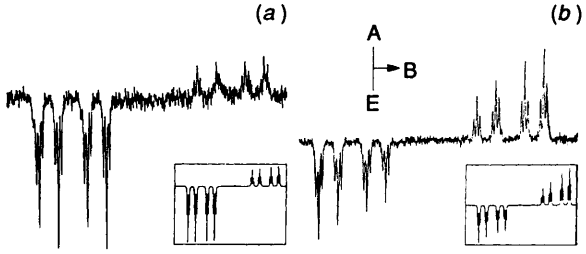

Figure 3. The spectrum of radical (**1**) observed on irradiation of a 0.3 mol dm^{-3} solution of diethyl maleate in the diethyl phosphite–di-tert-butyl peroxide mixture, (*a*) between 1.0–2.0 μs post the laser flash, and (*b*) between 2.0–7.0 μs. Both spectra show the effects of population transfer, but its contribution is greater at the earlier time. The simulated spectra are shown in the inserts. The sweep width was 12 mT.

their fast relaxation rates and their essentially instantaneous reaction with the phosphite present, Scheme 2.

$$Me_3C\text{–}O^{\bullet} + O = PH(OR)_2 \longrightarrow Me_3COH + O = P^{\bullet}(OR)_2,\ R = Me,Et$$

Scheme 2.

It is uncertain what the spin multiplicity of the excited state of the peroxide which dissociates is,[13] but in no circumstances have our, or previous,[14] experiments yielded spin polarization which can be attributed directly to the encounters of tert-butoxy radicals when they are known to be present in experimental systems. The spectrum of the phosphonyl radicals exhibits polarization which is consistent with it originating in the encounters of identical pairs of these phosphorus-centred radicals, which consequently can be viewed as the primary ones in the system where the polarization properties are concerned. Whether this should be viewed as resulting from a triplet geminate pair created by rapid radical substitution in the spin-correlated pair, or from an F-pair, is, luckily, immaterial where the qualitative polarization behaviour is concerned since both yield E/A patterns in the spectra. The spectra consist of doublets of wide spacing (70.8 and 69.8 mT for the dimethyl and diethyl compounds respectively) with small couplings to the protons (0.05 mT and <0.05 mT). The emissive low field line in the spectra of these primary radicals is invariably of higher absolute intensity than the high-field absorptive one due to the influence of ST_{-1} mixing.[9,10] An example is shown in Figure 2.

When an appropriate radical scavenger is added to the solution, the primary adds to a double bond to yield a secondary radical whose spectrum may reflect this polarization asymmetry to a greater or lesser extent, depending on the rates of various kinetic processes. At one extreme, if the primary polarization is allowed to build up to its fullest extent before reaction to form the secondary radical occurs, the low and high field regions in the spectrum of the latter would be expected to have relative intensities which corresponded directly to those in the phosphonyl radicals. However, distortions would be expected later in time due to additional F-pair polarizations possibly arising in both primary–secondary and secondary–secondary pairs. The greatest simplicity can be obtained by ensuring that the initial radical is entirely consumed by scavenger in the first microsecond of the reaction so that any polarization which occurs after the polarization transfer step is due to F-pair encounters of identical adduct radicals. The concentrations of scavengers required to meet this condition were determined empirically by monitoring of the intensities of the phosphonyl doublets in each system, as these concentrations were increased. Throughout all the experiments reported here observations made using diethyl phosphite in the reaction mixture mirrored those using the dimethyl compound completely.

A clear example of polarization transfer, but also of the complexities of the polarization behaviour observed in these systems, is provided by radical addition to diethyl maleate to give radical (**1**), Scheme 3.

$$EtO_2C = CCO_2Et + O = P^{\bullet}(OEt)_2 \longrightarrow$$

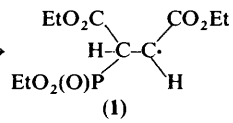

(**1**)

Scheme 3.

The spectra obtained at two different times after the photolysis flash are shown in Figure 3; the experimental details are included in the figure caption. Analysis shows that the coupling constants have the following values: $A_P = 6.89$ mT, $A_{\alpha H} = 2.03$ mT, $A_{\beta H} = 0.81$ mT (lower than usual due to the presence of the phosphorus-containing group), and $A_{\delta H} = 0.13$ mT. Figure 3 also shows the simulated spectrum obtained from an empirical admixture of contributions to line intensities from the polarization transfer process and from the RPM mechanism from F-pairs of identical adduct radicals. The former was calculated on the assumption that the complete population difference due to polarization in the primary in the absence of scavenger was carried to the secondary, and it reflects a strong ST_{-1} contribution to the spectrum. In the experimental spectrum obtained soon after radical formation, the transfer polarization dominates the observations and the spectrum calculated to fit the observed one was obtained by adding the two basic polarization contributions in the proportion of 5:1, transfer to RPM. The transfer contribution is however only produced at the time the secondary is formed, very quickly after the laser flash. The population difference due to it subsequently diminishes by spin–lattice relaxation, but F-pair RPM polarization continues to be created while reactive radicals (here the adducts) remain in the system. In the spectrum observed at the later time, therefore, the relative contributions from the two polarization mechanisms change, and the spectrum is now reproduced by adding them in the ratio 1:2. There are unfortunately too many unknown rate constants in the process concerned to interpret these proportions in a physical sense, and we rather use the simulations to confirm that the basic interpretation of the behaviour is as suggested above.

Careful inspection of the Figures shows that small discrepancies remain between the observed and calculated spectra. These result from hyperfine-dependent relaxation in the

Table.

		1 2 3	4 5 6	7 8 9	10 11 12
	m_α	−1/2	−1/2	+1/2	+1/2
	m_β	+1/2	−1/2	+1/2	−1/2
A_δ positive:	Σm_δ	10 − 1	10 − 1	10 − 1	10 − 1
A_δ negative:	Σm_δ	−101	−101	−101	−101

radicals. The study of this phenomenon has been recognized for some time as a possibility in the spectra of spin-polarized radicals,[15] but its application has been limited by the often strong intensity perturbations which result from RPM mechanism polarization and which tend to obscure more subtle effects. Here polarization transfer after the primary polarization step yields transitions of equal intensity in the spectrum of the secondary radical (if the degeneracies are equal) inside each half (low and high field) of the spectrum. This allows their individual evolution in time to be studied until F-pair effects subsequently distort the observations. The intensity changes are dominated by spin-lattice relaxation (although not entirely due to it [1]) and this may exhibit a hyperfine dependence according to the familiar general relation:[16–18]

$$\frac{1}{T_1} = a + bm_1 + cm_1^2 \qquad (1)$$

where m_1 is the total magnetic quantum number associated with a given hyperfine line, and a, b, and c are constants. They are given by the inner products of the traceless parts of the g-tensor, the g- and the A-tensor and the A-tensor respectively. When, as here, coupling occurs to more than one proton, or group of protons, this equation must be amended in a way originally discussed for T_2 processes by Carrington, Hudson, and Luckhurst:[19]

$$\frac{1}{T_1} = a + \sum_i b_i m_1(i) + \sum_i c_i m_1(i)^2 + \sum_{i<j} d_{ij} m_1(i) m_1(j) \qquad (2)$$

where the b_i and c_i parameters refer to each nucleus in turn, and d_{ij} is the inner product of the traceless parts of the hyperfine coupling tensors to the ith and jth nuclei.

The implication is that the relaxation times of lines in the spectrum corresponding to specific hyperfine states are expected to differ, and the lines may be identified from their relaxation behaviour, if the term linear in m_1, and/or the final term in equation (2), is significant. The assignment of these lines to specific hyperfine states depends upon the relative signs of the coupling constants, which can be determined in principle.[20] Unfortunately, the signs of the b and d parameters are not known in general, and this prevents us from obtaining a unique assignment in our system. However, we shall illustrate the approach to the analysis which may be possible.

We turn our attention to the low-field sub-spectrum due to hydrogen couplings shown in Figure 3. It consists of a major quartet of lines which originate in the couplings to the α and β protons, each member of which is split into a triplet by coupling to two equivalent δ protons. Inspection of the spectrum dominated by polarization transfer indicates that the lowest-field and third lowest-field lines of the quartet are of lower intensity, at the time the spectrum was recorded, than the other two; this indicates that these lines relax fastest. In the triplet sub-structure to these particular lines, the lower-field transition is more intense than the higher-field one; the converse is true for the other pair of lines in this quartet. This second feature is also apparent in the second spectrum in Figure 3 in which the effects of differential relaxation rates dominate those due to the slightly different RPM polarization of the components in the triplets. Once again, these observations reflect different relaxation rates of the triplet components.

To rationalize these observations we assume that A_α is negative, that A_β is positive, and that $|A_\alpha| > |A_\beta|$, as above. This leads to the identification of the lines with the specific spin states of the α and β protons listed in the Table. We then have two possible assignments of the lines in the triplet components, depending on whether A_δ is positive or negative. We consider first the major quartet splittings. It can be seen that the triplet of lines 1–3 corresponds to the β proton in its + 1/2 spin state, as does the triplet of lines 7–9, and these have similar rates of relaxation, faster than for the other two triplets, which result from radicals with β in its − 1/2 state. The observations are then consistent with the second term in equation (2) dominating the relaxation behaviour, and with the coefficient $|b_\beta| \gg |b_\alpha|$, and positive. This sign is consistent with A_β being taken as a positive quantity, provided that the g-tensor does not depart too strongly from cylindrical symmetry. We now consider the relative intensities of the triplet components, and may concentrate on the sub-ensemble of radicals in which the α proton has − 1/2 spin, that is on the two triplets 1–3 and 4–6, Table. Here it is immediately obvious that the second term in equation (2) cannot produce the situation wherein the high-field lines in each triplet relax at different rates, since these lines correspond to the same spin state of the δ proton. This is true, unfortunately, whether A_δ has either a positive or a negative sign. The different behaviours of lines are consequently due to the final, cross, term in equation (2), since the β proton has opposite spin states in the two triplets and causes this term to change in sign between the high-field lines in the two triplets. Further progress is impossible without knowing the sign of $d_{\beta\delta}$, but it might be conjectured that the sign of this inner product is determined by the signs of the couplings to the β and δ protons. In this case, with A_β known to be positive, a negative sign for A_δ would imply that $d_{\beta\delta}$ should be negative; the converse would be true for a positive value of this small coupling constant. Within the sub-ensemble of radicals selected, we may write the relaxation rate of lines 1 and 3, for example, as: $a^* + d_{\beta\delta}(-1/2)(\pm 1)$ for A_δ negative, and $a^* - d_{\beta\delta}(-1/2)(\pm 1)$ for A_δ positive, where the upper sign refers to line 1, and the lower to line 3, and a^* contains all the terms in equation (2) other than the cross-one. With $d_{\beta\delta}$ negative for A_δ negative, the former implies that the relaxation rate of line 1 should be less than that of line 3, as observed. However, this is also true for the alternative combination of $d_{\beta\delta}$ positive, and A_δ positive. We conclude that while we are able to understand the relaxation behaviour observed experimentally, we cannot obtain the sign of the coupling constant in the absence of an independent calculation of the sign of $d_{\beta\delta}$. Interestingly though, the two combinations in which A_δ and $d_{\beta\delta}$ might have opposite signs are incompatible with the observed behaviour. The observations are consequently consistent with the simple argument given above for a direct correlation in the signs of the two parameters A_δ and $d_{\beta\delta}$.

A similar discussion cannot be made of the phosphorus coupling since the relative intensities of the low- and high-field quartets are dominated by polarization, rather than relaxation effects, although we have some evidence for a different behaviour among the triplet components between the halves of the spectrum. However, the E/A pattern mimics that in the primary species, showing that the P-couplings have the same sign in each radical.

The spectra obtained using the dimethyl phosphite solution with added maleic anhydride and methyl maleic anhydride, and observed soon after the laser flash, are shown in Figures 4(*a*)

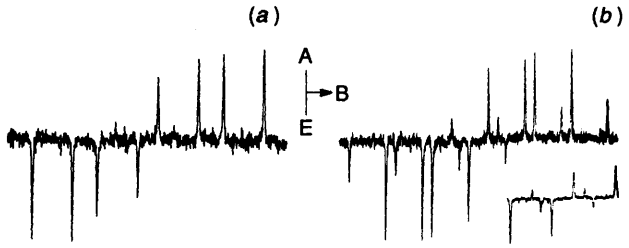

Figure 4. (*a*) The spectrum of radical (**4**) obtained on irradiation of a 0.5 mol dm^{-3} solution of maleic anhydride in the diethyl phosphite-containing stock solution and observed from 0.7–1.7 μs post flash. It is dominated by transfer polarization effects (see the text). The sweep width was 13.0 mT. (*b*) The corresponding spectrum, observed over the same time interval, of radical (**3**) from a 0.5 mol dm^{-3} solution of methyl maleic anhydride, observed with a sweep width of 17.0 mT. This too is dominated by polarization transfer, and now overlap of the proton subspectra causes a mixture of the phases of the transitions towards the centre of the spectrum. This is most clearly seen in the scale-expanded central region, observed over 6.0 mT, shown as an insert. Weak lines are seen also from radical (**2**) in the main spectrum.

and (*b*) respectively. Both correspond to radicals formed by addition of the primary phosphonyl radical to the double bond. The coupling constants are: in (**2**), A_P = 6.48 mT and $A_{\alpha H}$ = 1.84 mT (these are approximate values due to the low concentration of this species causing it to be observed with poor signal-to-noise ratio); in (**3**), A_P = 6.23, $A_{\alpha H}$ = 2.80, and A_{Me} = 2.21; in (**4**), A_P = 6.31, $A_{\alpha H}$ = 2.02, and $A_{\beta H}$ = 3.25 mT. In Figure

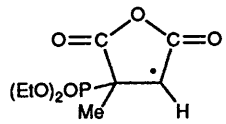

(**2**)

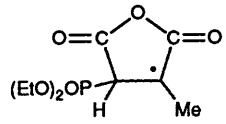

(**3**)

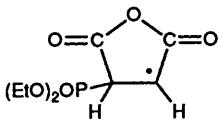

(**4**)

4(*a*), the occurrence of transfer polarization is shown by the strong central lines in the spectrum. It is noticeable that the spectrum lacks the strong emissive contribution of the corresponding one in Figure 2, which suggests that secondary radical formation is now so fast as to interfere with the full polarization development in the primary. However, this conclusion must be provisional, in a complex reaction system involving many possible polarization and relaxation routes.

The spectrum obtained from the methyl anhydride derivative is interesting in two aspects. Firstly, it shows an unmistakable manifestation of secondary polarization: lines of opposite phases are intermingled in the central region. This corresponds to the situation illustrated in Figure 1(*c*), and it occurs because the sum of the couplings to the protons exceed that to the phosphorus nucleus, and the two proton sub-spectra corresponding to the two spin states of the phosphorus nucleus overlap. Once again the spectrum exhibits little effect of transfer of ST_{-1} polarization from the primary radical, and also little contribution from ST_0 RPM effects. Secondly, the spectrum exhibits very weak lines due to radical (**2**), showing that the addition of the primary species is highly regiospecific due to steric hindrance from the methyl group. Since the spectrum is little affected by RPM polarization, it is possible to integrate the areas under the lines from each species to obtain a 2% abundance for the minor component. This is a valid comparison since both radicals are produced by addition of the identical, and identically polarized, primary species; it agrees well with a literature value obtained from a product analysis study.[5]

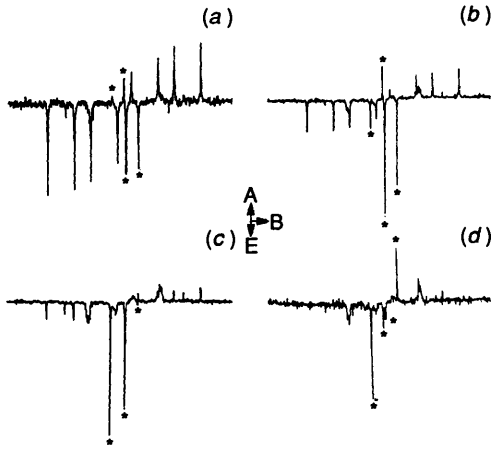

Figure 5. The time-evolution of the spectrum observed from the maleic anhydride system in the presence of a low concentration of base, with a sweep width of 17 mT, at the following times after the photolysis flash: (*a*) 0.5–2.0 μs, (*b*) 2.0–3.5 μs, (*c*) 3.5–5.0 μs and (*d*) 5.0–6.5 μs. Throughout, lines originating in radical (**3**) are evident, together with broader ones from oligomeric radicals and the photolysis of the products of reaction of anhydride with base. As time evolves the relative intensities of the lines from the adduct radical diminish as it becomes replaced by radical (**5**). The centre of the spectrum then shows the characteristic four line spectrum of this radical (marked with asterisks) initially in A/E phase. Thereafter, RPM polarization due to the encounters of like pairs of these radicals grows in and the phases of the lines change. This occurs because the transitions in the centre of the spectrum due to this form of polarization are weaker than the outside ones. In all of the spectra shown the amplitudes are normalized, and give no indication of the overall decay of the radical concentration in time.

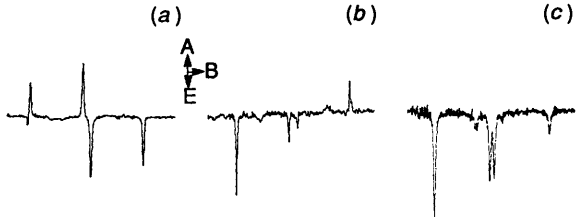

Figure 6. The central region of the spectra shown in Figure 5 observed, in the presence of 0.03 mol dm^{-3} sodium methoxide, at (*a*) 1.0–2.0 μs after the flash, when the spectrum of (**5**) exhibits essentially pure transfer polarization to give an A/E quartet with strong central lines, and at (*b*) 6.0–13.0 μs post flash when the spectrum has become dominated by an equilibrium signal distorted by E/A RPM polarization from pairs of identical tertiary radicals. In (*c*) is shown the very similar spectrum, in terms of line positions, from the identified radical (**6**). All spectra were recorded using a sweep width of 3.0 mT.

The spectra obtained when a low concentration of base (*ca.* 0.01 mol dm^{-3}) is added to the reaction mixture are considerably more complex and display the presence of further radicals whose concentrations rise and fall as time proceeds. This is illustrated in Figure 5. In the earliest spectrum, transitions from the adducts (**2**) and (**3**) are seen together with those from photolysis of the products of reaction of anhydride and base. Once again the relative intensities of the lines disclose that there is a dominant contribution from a polarization transfer process. As time proceeds, the intensities of the adduct spectra diminish as they disappear chemically and they become progressively replaced by a further species which shows a simple and narrow four-line spectrum. This is most clearly seen in the enlarged central region shown in Figure 6. At the earliest time after the

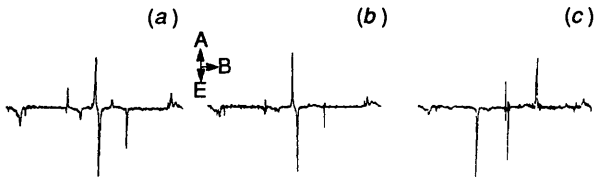

Figure 7. The central region of the spectrum observed with similar conditions to those described above at 2.0–3.0 μs post flash, (*a*) in the presence of a trace of boric acid, (*b*) with no addition of acid or base, and (*c*) in the presence of 0.03 mol dm^{-3} sodium methoxide. At this time the spectrum in the acid solution still exhibits dominant polarization transfer behaviour, in the 'neutral' solution growing-in F-pair RPM polarization causes the outer lines to begin to change phase, and in the basic solution this process has gone much further, with the outer lines now in opposite phase from those observed in (*a*) and (*b*). The central and outer lines differ in their temporal behaviour due to the quite different characteristics of the two forms of polarization which contribute to the spectrum. Also of interest are the composite lineshapes observed as some of the lines change phase.[1] The sweep width was 6.0 mT.

laser flash that this spectrum can be clearly observed it exhibits, very interestingly, A/E polarization; that is an opposite sense of polarization from that in the spectrum of the adduct radical from which it is apparently formed [Figure 6(*a*)]. This is a very remarkable observation, for the species is evidently not a primary radical but if it was mistaken for one (for example by failing to take an early-time spectrum which shows its slow formation compared with other radicals present) it would be interpreted as showing that the species was formed from a singlet state precursor. This is the first example known in which a simple analysis made on a spectrum obtained at short observation times after radical formation, on the basis of the simple rules of CIDEP, would give an erroneous conclusion. The spectra in Figures 5 and 6 are once more dominated by polarization-transfer behaviour, as can be seen from the relatively high intensities of the central lines.

This is a significant observation, for it means that the polarization behaviour in the radicals does originate in the chemistry we have described, that is in the addition of a polarized primary radical to the substrate. Any addition of the phosphonate anion derived from the phosphite in the presence of base to maleic anhydride before illumination, with subsequent photolysis of the product, does not produce the polarized radicals that we observe.

As time goes on, normal F-pair RPM polarization grows in, and it quickly causes the outer two lines to show characteristic E/A phase, but the RPM contribution to the central lines is smaller (due to the $Q^{1/2}$-dependence of intensities), and these lines remain in their original phases longer. These changes can be monitored as they occur, and when the polarization transferred has relaxed, a normal E/A pattern is observed, and eventually a significant contribution from equilibrated radicals causes a single-phase spectrum to be obtained; the approach of this situation is shown in Figure 6(*b*). At certain times after the flash successive lines appear with E/A/E/A polarizations.

It remains to identify the radical, and an initial indication is obtained by studying the behaviour in the presence of varying concentrations of base: as the base concentration is increased the rate of formation of the radical is accelerated (Figure 7). This is best seen by following the polarization behaviour once more: in spectra recorded during the same time interval after radical formation, increase of base concentration causes the RPM contribution to the spectrum to increase, indicating that the radicals are formed more quickly. This represents a novel use of the time-dependence of a polarized spectrum to gain kinetic information on a timescale in which it cannot be obtained by monitoring the change of the radical concentration. These experiments indicate that the radical may result from proton loss by the adduct initially formed, and the only labile hydrogen is that attached to the phosphonyl carbon atom. The resulting radical is believed to be an anion which can exist in tautomeric forms. The measured couplings are 0.9 and 1.13 mT, which

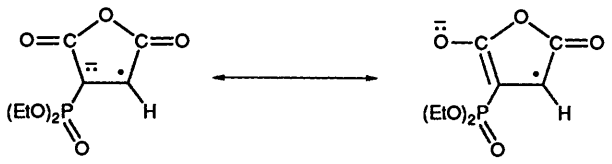

(5)

might both seem small for one of them to be to a phosphorus nucleus. However, a small coupling is consistent with theoretical predictions for radicals of similar structure.[21] To confirm the assignment, a closely related, although neutral, radical was created by an alternative route. Thus, photolysis of di-*tert*-butyl peroxide in the presence of diethyl phosphite (added to keep conditions similar to those in the above experiments) in a solution saturated with triphenylphosphoranylidene succinic anhydride yielded the spectrum shown in Figure 6(*c*). It consists of a similar quartet to that shown in the spectrum of the radical observed in the maleic anhydride solution, with couplings of 0.987 and 1.063 mT. The radical is formed by simple hydrogen abstraction of one of the hydrogens α to one carbonyl group, and has the unequivocal structure (**6**). By comparison with the

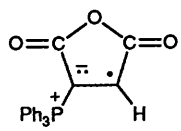

(6)

couplings observed in radical (**5**), we tentatively assign the smaller coupling to the α-H nucleus, and the larger to the coupling to the phosphorus nucleus. The spin polarization observed in the spectrum shown in Figure 6(*c*) results from the creation of both the phosphoranylidene radical and the phosphonyl one (from the phosphite present) following photolysis of the peroxide, and their subsequent encounter; it is dominated by a contribution from ST_{-1} mixing which causes the spectrum of (**6**) to appear wholly in emission, although an intensity contribution from an ST_0 effect is also apparent. This constitutes an unusual example of ST_{-1} effects in an F-pair polarization process.

Having determined the nature of the radical, and realizing that it is a secondary species within the meaning of this paper (it is actually in chemical terms a quaternary one, and in polarization terms a tertiary one), we return to the significance of it exhibiting an A/E polarization behaviour when first observed. As argued above, this polarization is clearly of transfer type, and the phase indicates that a correlated coupling has changed in sign between the precursor adduct radical and this one. This is most likely to be the phosphorus coupling since the geometry of the intervening carbon atom changes on proton abstraction. This is the first example of such a phase inversion, and the first example of a comparison of signs of coupling constants in different radicals which shows them to be opposite to one another. Such phase changes are also of potential use in tracking of radical reaction pathways. Indeed the whole of the work reported here has demonstrated the great power of flash-photolysis ESR observations in providing this type of mechanistic detail, with each successive species fully identified from its spectrum and its relation to its predecessor established from the CIDEP behaviour.

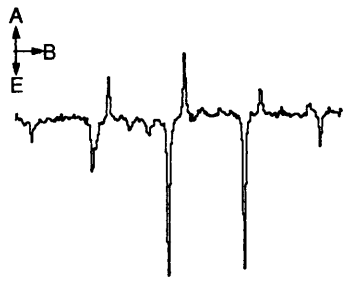

Figure 8. The spectrum of the tertiary radical (7) observed under similar conditions to those described above, in the presence of 0.03 mol dm^{-3} sodium methoxide, at 1.0–2.0 μs post flash; the sweep width was 4.5 mT. It consists of two quartets, due to coupling to the methyl protons, centred at the resonance positions of the two phosphorus hyperfine lines. As with the previous example, the transfer polarization is of A/E form, although at the time this spectrum was taken an RPM F-pair contribution already causes the lowest-field member of the lower-field sub-quartet to appear in emission.

Solutions containing methyl maleic anhydride in the presence of ethyl phosphite exhibit similar behaviour in that the initially formed adduct changes in time to a species with a spectrum consisting of four lines due to coupling to the methyl group further split by a coupling to phosphorus, Figure 8. By analogy with the above we assign the following structure to the radical (7). In this spectrum, the two methyl subspectra centred at

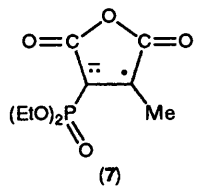

(7)

the resonance positions of the individual spin states of the phosphorus nucleus appear in opposite phases, and the overall behaviour is A/E, with the quartet centred at the lower field in absorption. Not surprisingly, this behaviour is entirely analogous to that described above. The magnitudes of the couplings were A_{Me} = 2.06 and A_p = 1.64 mT.

In experiments conducted using dimethylmaleic anhydride, the adduct radical was observed, with couplings of A_p = 6.76 and A_{Me} = 2.25 mT. Its spectrum was also dominated by polarization transfer effects and, as previously, it exhibited E/A polarization, indicating similar signs of coupling constants between the parent phosphonyl and daughter adduct radicals. In this case, however, no tertiary radical was observed. This is as expected from the absence of a labile hydrogen in the molecule, and it adds credence to the assignment made above.

Finally, we turn to the purely chemical implications of this work. The tertiary radical is very similar to a carbanion which has been widely used in the Horner–Emmons modification of the Wittig reaction.[22] Without undertaking specific kinetic studies, the ESR spectra of transient radicals obtained in this study have been used to provide physical and chemical information on this system; a full kinetic analysis of the spectra of the tertiary radicals is, however, underway. In a similar way, it should be possible to introduce ketones into the reaction mixture, and to use the adjacent radical centre as a, hopefully, non-intrusive label during the Wittig reaction.

Acknowledgements

We thank Michel Geoffroy for helpful discussions on the sizes of the phosphorus couplings, and the SERC for their support.

References

1 K. A. McLauchlan, in 'Advanced EPR, applications in Biology and Biochemistry,' ed. A. J. Hoff, Elsevier, 1989, p. 345.
2 C. D. Buckley, A. I. Grant, K. A. McLauchlan, and A. J. D. Ritchie, *J. Chem. Soc., Faraday Trans.*, 1984, **78**, 251.
3 J. B. Pedersen, *FEBS Lett.*, 1979, **97**, 305.
4 K. A. McLauchlan, in 'Chemically Induced Magnetic Polarization,' eds. L. T. Muus, P. W. Atkins, K. A. McLauchlan, and J. B. Pedersen, Reidel, Dordrecht, 1977, p. 151.
5 B. Giese and G. Kretzschmar, *Chem. Ber.*, 1984, **117**, 3175.
6 P. J. Hore and K. A. McLauchlan, *Mol. Phys.*, 1981, **42**, 533.
7 K. A. McLauchlan and D. G. Stevens, *Chem. Phys. Lett.*, 1985, **115**, 108.
8 K. A. McLauchlan and N. J. K. Simpson, *Chem. Phys. Lett.*, 1989, **154**, 550.
9 C. D. Buckley and K. A. McLauchlan, *Chem. Phys. Lett.*, 1987, **137**, 86.
10 T. J. Burkey, J. Lusztyk, K. U. Ingold, J. K. S. Wan, and F. J. Adrian, *J. Phys. Chem.*, 1985, **89**, 4286.
11 F. J. Adrian, *J. Chem. Phys.*, 1971, **54**, 3918.
12 S. Basu, K. A. McLauchlan, and G. R. Sealy, *J. Phys. (E) Sci. Instrum.*, 1983, **16**, 1767.
13 F. H. Dorer and S. N. Johnson, *J. Phys. Chem.*, 1971, **75**, 3651.
14 M. C. Thurnauer, T-M. Chiu, and A. D. Trifunac, *Chem. Phys. Lett.*, 1985, **116**, 543.
15 K. A. McLauchlan and D. G. Stevens, *Mol. Phys.*, 1987, **60**, 1159.
16 P. W. Atkins and D. Kivelson, *J. Chem. Phys.*, 1966, **44**, 169.
17 P. S. Hubbard, *Phys. Rev.*, 1963, **131**, 1155.
18 G. Nyberg, *Mol. Phys.*, 1967, **12**, 69.
19 A. Carrington, A. Hudson, and G. R. Luckhurst, *Proc. R. Soc., London, Sect. A*, 1965, **284**, 582.
20 E. De Boer and E. L. Mackor, *J. Chem. Phys.*, 1963, **38**, 1450.
21 Dr. Michel Geoffroy, personal communication.
22 J. Bautagy and R. Thomas, *Chem. Rev.*, 1974, **74**, 87.

Paper 9/05515K
Received 28*th December* 1989
Accepted 24*th April* 1990